A Feasibility Analysis at Signal-Free Intersections

Filippos N. Tzortzoglou, *Student Member, IEEE*, Logan E. Beaver, *Member, IEEE*, and Andreas A. Malikopoulos, *Senior Member, IEEE*

***Abstract*—In this letter, we address the problem of improving the feasible domain of the solution of a control framework for coordinating connected and automated vehicles (CAVs) at signal-free intersections. The framework provides the optimal trajectories of CAVs to cross the intersection safely without stop-and-go driving. However, when traffic volume exceeds a certain level, finding a feasible solution for a CAV may become unattainable. We use concepts from numerical mathematics to identify appropriate polynomials that can serve as alternative trajectories of the CAVs, expanding the domain of the feasible CAV trajectories. We then select the final trajectories through an optimization problem that aims at minimizing jerk. Finally, we demonstrate the efficacy of our approach through numerical simulations.**

***Index Terms*—Connected automated vehicles, traffic flow, and interpolation.**

I. Introduction

IN RECENT decades, society has witnessed commendable efforts towards improving emerging mobility systems [1]. One significant sector of this improvement is associated with the use of connected and automated vehicles (CAVs) [2]. It has been shown that the use of CAVs can lead to a safer traffic network, improve fuel consumption, and maximize throughput on the roads [3]. Several research efforts have provided approaches on how CAVs can create a more sustainable traffic network [4]. Adaptive cruise control and cooperative adaptive cruise control have been extensively discussed in the literature [5]. These approaches allow for a vehicle to define its speed/orientation trajectories according to the environment in which it exists. Attention has been given to ecological adaptive cruise control [6], which also considers environmental aspects.

Studies have shown that a crucial reason for bottlenecks in the U.S. is associated with congestion on merging on-ramps, intersections, and roundabouts [7]. Many researchers have investigated how CAVs can contribute to such scenarios using different kinds of approaches like time-optimal control strategies [8], [9], reinforcement learning [10], [11] and model predictive control [12], [13].

However, challenges have emerged in optimal control strategies when unconstrained solutions are infeasible, necessitating non-real-time processes such as piecing together constrained and unconstrained arcs. From a theoretical point of view, in [14] and [15], the authors discuss that state-constrained continuous-time optimization is an intractable and difficult problem to solve. From the application point of view, in [16], the authors proposed a controller for coordinating CAVs on merging ramps, highlighting the computational obstacles of constrained solutions. Conditions that ensure feasible unconstrained trajectories were presented in [17] and [18], underscoring the impracticality of constrained ones. The importance of enhancing feasibility was emphasized in [8] whereas piecing together arcs is also necessary in [9]. To the best of our knowledge, there is no existing approach in the literature that avoids piecing together arcs while minimizing energy consumption when no feasible unconstrained solution exists.

In this letter, we analyze the decentralized control framework reported in [19] and address its limitations related to operating feasibility. The framework provides the optimal time trajectory for each CAV that arrives at an intersection's control region. When no feasible unconstrained solution exists, we introduce an alternative approach that enables CAVs to determine their trajectories online. Our approach extends the problem formulation in [19], which confines the optimal unconstrained trajectory to a third order polynomial. By recognizing that a third order polynomial solution can be restrictive, employing a higher order polynomial may facilitate the identification of an unconstrained trajectory. Using concepts from numerical mathematics, we show that any CAV entering the intersection can extend its range of feasible solutions by interpolating a polynomial that describes its position trajectory. Nonetheless, given the potential for multiple trajectory solutions, our approach prioritizes the trajectory that minimizes jerk, thus optimizing not only energy efficiency but also passenger comfort. Moreover, we demonstrate the feasibility of solving this optimization problem online, enabling real-time trajectory planning for vehicles. This letter contributes in the field by:

(1) Providing an intersection coordination scheme that handles CAVs trajectories using polynomial interpolation.

(2) Proposing a control framework for managing CAVs at signal-free intersections, increasing the feasibility domain when unconstrained optimal solutions are unattainable.

(3) Establishing an optimization problem that facilitates the real-time determination of optimal CAV trajectories.

The remainder of this letter proceeds as follows. In Section II, we introduce the problem formulation. In

Manuscript received 8 March 2024; revised 9 May 2024; accepted 23 May 2024. Date of publication 6 June 2024; date of current version 15 August 2024. This work was supported by NSF under Grant CNS-2149520 and Grant CMMI-2219761. Recommended by Senior Editor C. Manzie. *(Corresponding author: Filippos N. Tzortzoglou.)*

Filippos N. Tzortzoglou and Andreas A. Malikopoulos are with the School of Civil and Environmental Engineering, Cornell University, Ithaca, NY 14853 USA (e-mail: ft253@cornell.edu; amaliko@cornell.edu).

Logan E. Beaver is with the Department of Mechanical and Aerospace Engineering, Old Dominion University, Norfolk, VA 23529 USA (e-mail: lbeaver@odu.edu).

Digital Object Identifier 10.1109/LCSYS.2024.3410629

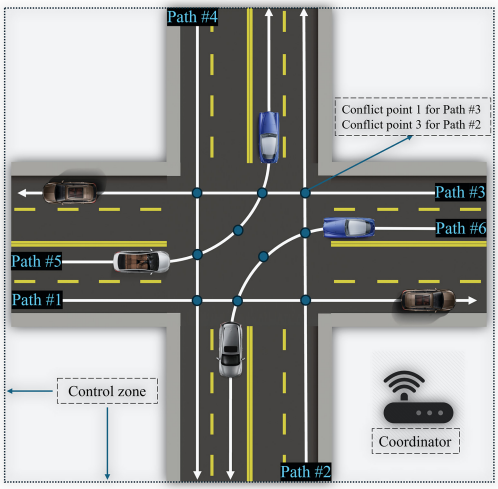

Fig. 1. Schematic of the intersection showing the control zone, conflict points, and paths.

Section III, we provide our approach, and in Section IV, we provide numerical simulations. Finally, in Section V, we draw some concluding remarks.

II. Problem Formulation

We consider a signal-free intersection illustrated in Fig. 1. Although this letter's theoretical framework is applicable to various traffic scenarios, we focus on intersections, excluding right turns, to highlight the unique technical challenges associated with a larger number of conflicting paths. A coordinator handles communication with the CAVs within a given range. We call this communication region *control zone*. In our formulation, we consider that CAVs do not perform any lane-change maneuver. Thus, there exists a finite number of paths within the control zone. These paths constitute the set $\mathcal{L} = \{1, 2, \ldots, z\}$, $z \in \mathbb{N}$. The points where the roads intersect and lateral collisions may occur are called conflict points and belong to the set $\mathcal{O}_z \subseteq \mathbb{N}$ for each $z \in \mathcal{L}$. The set $\mathcal{N}(t) = \{1, 2, \ldots, N(t)\}$ denotes the queue of vehicles inside the control zone at time t, where $N(t)$ denotes the total number of vehicles at time t.

We consider that the dynamics of each CAV $i \in \mathcal{N}(t)$ are described by a double integrator model, i.e.,

$$\begin{aligned} \dot{p}_i(t) &= v_i(t), \\ \dot{v}_i(t) &= u_i(t), \end{aligned} \tag{1}$$

where $p_i \in \mathcal{P}$, $v_i \in \mathcal{V}$, and $u_i \in \mathcal{U}$ denote the longitudinal position of the rear bumper, speed, and control input (acceleration) of the vehicle, respectively. The sets $\mathcal{P}$, $\mathcal{V}$, and $\mathcal{U}$ are compact subsets of $\mathbb{R}$. The control input is bounded by

$$u_{i,\min} \leq u_i(t) \leq u_{i,\max}, \quad \forall i \in \mathcal{N}(t), \tag{2}$$

where $u_{i,\min} < 0$ and $u_{i,\max} > 0$ are the minimum and maximum control inputs, respectively, as designated by the physical acceleration and braking limits of the vehicles, or the limits of passenger comfort, whichever is more restrictive. Next, we consider the speed limits,

$$v_{\min} \leq v_i(t) \leq v_{\max}, \quad \forall i \in \mathcal{N}(t), \tag{3}$$

where $v_{\max} > v_{\min} > 0$ are the maximum and minimum allowable speeds. This implies that a CAV is not allowed to stop within the intersection.

A. Safety Constraints

Let p_i^0 be the entry point in the intersection of each CAV i, p_i^n be the position at the conflict point $n \in \mathcal{O}_z = \{1, 2, 3\}$ (note that each path z in Fig. 1 passes through 3 conflict points), and p_i^f be the exit point of the intersection. Let $t_i^0 \in \mathbb{R}_{\geq 0}$ be the time at which CAV i enters the control zone and $t_i^n \in \mathbb{R}_{\geq 0}$ be the time at which it reaches the conflict point $n \in \{1, 2, 3\}$; and let $t_i^f \in \mathbb{R}_{\geq 0}$ be the time when it exits the control zone.

Since the speed $v_i(t)$ is bounded below by a positive number $v_{\min} > 0$, the position $p_i(t)$ monotonically increases leading to an injective (one-to-one) position trajectory function. Thus, the inverse function exists and corresponds to the time trajectory defined as $t_i(p) = p_i^{-1}(t)$, which allows us to determine t_i^n, the time at which CAV i arrives at conflict point n. Note that the constraint $v_{\min} > 0$ can be relaxed to allow $v_i(t) \geq 0$ by considering the pre-image of $p(t)$ instead of the inverse in the following analysis.

To avoid conflicts between vehicles in the control zone, we need to impose the following safety constraints: (1) the rear-end constraints between vehicles on the same path and (2) the lateral safety constraints between vehicles traveling on different intersecting paths. To ensure rear-end collision avoidance between a CAV $i \in \mathcal{N}(t)$ and its leading CAV $k \in \mathcal{N}(t) \setminus \{i\}$, we impose that

$$t_i(p) - t_k(p) \geq \tau_r, \tag{4}$$

where τ_r denotes a safe time headway between two consecutive vehicles. For lateral collision avoidance, we consider a scenario where CAV $k \in \mathcal{N}(t) \setminus \{i\}$ has a planned trajectory potentially leading to a conflict with CAV i. In such a scenario, we need to investigate the two following cases:

Case 1. CAV i reaches the conflict point n^* after CAV k. Then, we require

$$t_i^{n^*} - t_k(p) \geq \tau_\ell \quad \forall p \in \left[p_k^0, p_k^{n^*}\right], \tag{5}$$

where $t_i^{n^*}$ denotes the time CAV i arrives at conflict point n^* and t_ℓ denotes the lateral safe time headway. This constraint ensures CAV i must reach conflict point n^*, t_ℓ seconds after CAV k crosses the point. Note that in order to avoid ambiguity, we denote the conflict point as n^* to showcase that we refer to the common conflict point for each path.

Case 2. CAV i arrives at conflict point n before CAV k. Then, we require

$$t_k^{n^*} - t_i(p) \geq \tau_\ell \quad \forall p \in \left[p_i^0, p_i^{n^*}\right]. \tag{6}$$

Next, we review the optimal trajectory of a CAV i by using the two-level optimization framework presented in [19]. The upper-level framework focuses on determining, for every CAV $i \in \mathcal{N}(t)$, the shortest possible time t_i^f to exit the control zone, given its desired destination. The low-level framework involves an optimization problem, the solution of which derives the optimal control input for CAV $i \in \mathcal{N}(t)$, given t_i^f, while adhering to constraints related to the vehicle's constraints.

B. Low-Level Optimization

We start our exposition by reviewing the framework presented in [19] that aims at deriving the energy-optimal trajectory for each CAV i. We consider that for every CAV $i \in \mathcal{N}(t)$, the time t_i^f (exiting time of the control zone) is known. Then, the energy-optimal control problem finds the optimal input by solving the following optimization problem.

Problem 1 (Energy-Optimal Control Problem):

$$\begin{aligned}&\min_{u_i\in\mathcal{U}} \quad \frac{1}{2}\int_{t_i^0}^{t_i^f} u_i^2(t)\,\mathrm{d}t,\\ &\text{subject to:} \quad (1),\ (2),\ (3),\ (4),\ (5),\ (6),\\ &\text{given:} \quad p_i\left(t_i^0\right)=p_i^0,\ v_i\left(t_i^0\right)=v_i^0,\ p_i\left(t_i^f\right)=p_i^f,\end{aligned} \tag{7}$$

where v_i^0 is the speed of CAV i at t_i^0. The boundary conditions in (7) are set at the entry and exit of the control zone.

The closed-form solution of this problem for each CAV i can be derived using the Hamiltonian analysis as presented in [19]. The optimal unconstrained trajectory is as follows:

$$\begin{aligned}u_i(t) &= 6\phi_{i,3}t + 2\phi_{i,2},\\ v_i(t) &= 3\phi_{i,3}t^2 + 2\phi_{i,2}t + \phi_{i,1},\\ p_i(t) &= \phi_{i,3}t^3 + \phi_{i,2}t^2 + \phi_{i,1}t + \phi_{i,0},\end{aligned} \tag{8}$$

where $\phi_{i,3}, \phi_{i,2}, \phi_{i,1}, \phi_{i,0}$ are constants of integration. Given the boundary conditions in Problem 1, the optimal boundary condition $u_i(t_i^f)=0$ and considering t_i^f is known, the constants of integration can be found by:

$$\boldsymbol{\phi}_i = \begin{bmatrix}\phi_{i,3}\\ \phi_{i,2}\\ \phi_{i,1}\\ \phi_{i,0}\end{bmatrix} = \begin{bmatrix}\left(t_i^0\right)^3 & \left(t_i^0\right)^2 & t_i^0 & 1\\ 3\left(t_i^0\right)^2 & 2t_i^0 & 1 & 0\\ \left(t_i^f\right)^3 & \left(t_i^f\right)^2 & t_i^f & 1\\ 6t_i^f & 2 & 0 & 0\end{bmatrix}^{-1}\begin{bmatrix}p_i^0\\ v_i^0\\ p_i^f\\ 0\end{bmatrix}. \tag{9}$$

Having defined Problem 1, we are ready to present the upper-level optimization problem, where we compute t_i^f, which is then passed as an input to Problem 1.

C. Upper-Level Optimization Problem

Problem 2 (Time-Optimal Control Problem): At the time t_i^0 of entering the control zone, let $\mathcal{F}_i(t_i^0)=[\underline{t}_i^f, \bar{t}_i^f]$ be the feasible range of travel time under the state and input constraints of CAV i computed at t_i^0. The values $\underline{t}_i^f$ and $\bar{t}_i^f$ can be found by letting the CAV accelerate or decelerate at the maximum rate, respectively. Then CAV i solves the following time-optimal control problem to find the minimum exit time $t_i^f \in \mathcal{F}_i(t_i^0)$ that satisfies all the constraints:

$$\begin{aligned}&\min_{t_i^f\in\mathcal{F}_i(t_i^0)} \quad t_i^f\\ &\text{subject to:} \quad (1),\ (2),\ (3),\ (4),\ (5),\ (6)\\ &\text{given:} \quad p_i\left(t_i^0\right)=p_i^0, v_i\left(t_i^0\right)=v_i^0, p_i\left(t_i^f\right)=p_i^f, u_i\left(t_i^f\right)=0\end{aligned}$$

The computation steps for numerically solving Problem 2 are summarized as follows. First, we initialize $t_i^f=\underline{t}_i^f$, and compute the parameters ϕ_i using (9). We evaluate all the state, control, and safety constraints. If none of the constraints is violated, we return the solution; otherwise, t_i^f is increased by a step size. The procedure is repeated until the solution satisfies all the constraints.

Finally, by solving Problems 1 and 2, the optimal exit time t_i^f along with the optimal trajectory and control law (13) are obtained for CAV i for $t\in[t_i^0, t_i^f]$.

Remark 1: In case a solution to Problem 2 does not exist due to congestion, we derive the optimal trajectory for the CAVs by piecing together the constrained and unconstrained arcs until the solution does not violate any constraints. However, piecing together arcs is rather computationally expensive. So, in Section III, we circumvent this issue using the concept of polynomial interpolation.

III. Enhancing the Domain of Feasible Solutions

In this section, we present an approach that enhances the CAV trajectories' feasible domain resulting from the solution of Problem 1. The position trajectories provided by Problem 1 are energy-optimal but constrained to be third order polynomials. Following, we relax this constraint and allow the position trajectories to be higher-order polynomials.

A. Theoretical Results

In this subsection, we provide some theoretical results needed for our analysis. We begin with Lemma 1, which demonstrates that using a higher-order polynomial can have valuable impacts on the position trajectory.

Lemma 1: A n^{th} order polynomial for $n>3$ can have 2 changes in the curvature of the position trajectory.

Proof: Consider $p(t)=a_nt^n+a_{n-1}t^{n-1}+\cdots+a_1t^1+a_0t^0$. Then $p'(t)=na_nt^{n-1}+(n-1)a_{n-1}t^{n-2}+\cdots+a_1$ and $p''(t)=n(n-1)a_nt^{n-2}+(n-1)(n-2)a_{n-1}t^{n-3}+\cdots+2a_2$. For $n>3$, $p''(t)$ is at least a second-order polynomial that can obtain 2 roots. However, the roots of $p''(t)$ define the changes in curvature of $p(t)$. This completes the proof. ■

Lemma 1 not only underlines that the position trajectory is capable of undergoing two changes in curvature but also shows that a higher order polynomial allows for non-linear acceleration since $p''(t)$ can be a second order polynomial. Moreover the speed trajectories can change slope sign two times. Such a property significantly impacts feasibility performance, as we will highlight in the simulation results.

Next, we introduce some results that enable the use of polynomial interpolation to define vehicle trajectories.

Theorem 1: Given $n+1$ distinct nodes, $\{x_0,\ldots,x_n\}$ and $n+1$ corresponding values $\{y_0,\ldots,y_n\}$, there exists a unique polynomial $f(x)$ of degree n, such that $f(x_i)=y_i$ for all $i=1,\ldots,n+1$.

Proof: See [20, p. 334, Th. 8.1]. ■

Theorem 2: The coefficients of a n^{th} order polynomial given n points are given by the following equation where the square matrix is a Vandermonde matrix:

$$\begin{bmatrix}1 & x_0 & x_0^2 & \cdots & x_0^{n-1}\\ 1 & x_1 & x_1^2 & \cdots & x_1^{n-1}\\ \vdots & \vdots & \vdots & \ddots & \vdots\\ 1 & x_{n-1} & x_{n-1}^2 & \cdots & x_{n-1}^{n-1}\end{bmatrix}\begin{bmatrix}\phi_0\\ \phi_1\\ \vdots\\ \phi_{n-1}\end{bmatrix} = \begin{bmatrix}y_0\\ y_1\\ \vdots\\ y_{n-1}\end{bmatrix} \tag{10}$$

Proof: See [21, Ch. 2, eq. (5)]. ■

To exploit the results provided by Theorems 1 and 2, we need to ensure that the Vandermonde matrix is invertible, which is not guaranteed in general since it depends on the values $x_0,\ldots,x_{n-1}$. The following result shows that a Vandermonde matrix has a specific determinant form. This specific form will assist us in proving that the Vandermonde matrix, as defined in (10), is invertible.

Lemma 2: The determinant of a $n\times n$ Vanderomonde matrix is equal to $\det(V)=\prod_{0\le i<j\le n-1}(x_j-x_i)$.

Proof: We use mathematical induction to prove this result. For $n=2$, we have $\det(V)=(x_1-x_0)$. For an $n\times n$ matrix (as

in (10)), we subtract from each column, the preceding column multiplied by x_0, starting from the last one. So, we get $V =$

$$\begin{bmatrix} 1 & 0 & 0 & 0 \\ 1 & x_1 - x_0 & x_1^2(x_1 - x_0) & x_1^{n-1}(x_1 - x_0) \\ 1 & x_2 - x_0 & x_2^2(x_2 - x_0) & x_2^{n-1}(x_2 - x_0) \\ 1 & x_{n-1} - x_0 & x_{n-1}^2(x_{n-1} - x_0) & x_{n-1}^{n-1}(x_{n-1} - x_0) \end{bmatrix} \quad (11)$$

Then, the determinant of our matrix is equal to the determinant of the sub-matrix below the zeros, which can be simplified by factoring out the terms $(x_1 - x_0), \ldots, (x_{n-1} - x_0)$. Therefore, $\det(V) = \prod_{1 \le j \le n-1}(x_j - x_0)V'$, where V' is the remaining matrix, which is still a Vandermonde matrix. Following the same process iteratively for V', we will end up with a 2×2 Vandermonde matrix, which completes the induction. ■

Next, we prove that the determinant provided in Lemma 2 is not equal to zero. Given the nature of our application, we consider that the values $x_0, \ldots, x_{n-1}$ represent times along a CAV's trajectory, and $y_0, \ldots, y_{n-1}$ represent the corresponding positions. Then, having known that the time trajectory is strictly increasing, it is sufficient to show that the matrix is invertible if $0 < x_0 < x_1 < \ldots < x_{n-1}$. Let us prove that in the following theorem.

Theorem 3: The Vandermonde matrix presented in (10) is an invertible matrix if $0 < x_0 < x_1 < \ldots < x_{n-1}$.

Proof: From Lemma 1, the determinant of a Vandermonde matrix V is $\det(V) = \prod_{0 \le i < j \le n-1}(x_j - x_i)$. Since $x_0 < x_1 < \ldots < x_{n-1}$, it follows that for all i, j with $0 \le i < j \le n-1$, we have $x_j - x_i \neq 0$. Therefore, $\prod_{0 \le i < j \le n-1}(x_j - x_i) \neq 0$. A non-zero determinant implies that the matrix V is invertible and the proof is complete. ■

B. Implementation in CAVs

Next, we apply the results above to improve the operational feasibility of the controller. Consider a CAV i that cannot find a feasible trajectory after solving Problems 1 and 2. Then we aim to construct a n^{th} order polynomial using Theorems 1, 2, and 3, which corresponds to a feasible position trajectory $p(t)$ of CAV i, as defined in (1). In other words, our objective is to identify n points (t_i, p_i) along the trajectory of CAV i to interpolate. These nodes enable the use of (10) and must ensure that the resulting solution adheres to all constraints.

We choose to construct a fourth order polynomial, inspired by the fact that we already know the location of the position nodes $p_i^0, p_i^1, p_i^2, p_i^3$, and p_i^f. Given that we know these position nodes, we are searching for the corresponding times t_i^1, t_i^2, t_i^3, and t_i^f such that we can compute the coefficients ϕ_i of the fourth order polynomial using (10). Recall that t_i^0 is considered known, as it represents the time of entry into the control zone.

Remark 2: Note that our approach generalizes the third order polynomial solution and can yield solutions in a broader case of traffic scenarios. Furthermore, for systems with n^{th} order integrator dynamics, the control-minimizing trajectory is a $2(n-1)$ order polynomial [22]. Thus, we impose a smoother trajectory, minimizing energy consumption, and effectively handling the trade-off between passenger comfort and energy efficiency.

Next, we discuss how our approach can address lateral and rear-end constraints.

C. Lateral Constraints

In Section II.A, we pointed out that the lateral constraints for every CAV i are only associated with the points $(t_i^1, p_i^1), (t_i^2, p_i^2), (t_i^3, p_i^3)$. However, to interpolate from appropriate times t_i^1, t_i^2, and t_i^3 for a CAV i on path $z \in \mathcal{L}$, it is essential to ensure that there is always a non-empty set in which t_i^1, t_i^2, and t_i^3 can belong to. Namely, we want to show that for any path $z \in \mathcal{L}$, there is a sufficiently large gap between two vehicles at each conflict point such that a CAV from a conflicting path can safely pass between them. Next, we provide a condition for the existence of such a gap.

Algorithm 1 Selection of $\mathcal{T}_i^{n*}\ \forall\, n \in 1, 2, 3$ for CAV i

Ensure: Selection of an efficient $\mathcal{T}_i^{n*}$ for all $n \in \{1, 2, 3\}$
  for each $n \in \{1, 2, 3\}$ **do**
    for each disjoint set $\mathcal{T}_{i,j}^n \in \mathcal{T}_i^n, j \in \mathcal{D}^n$ **do**
      $t_{i,j,\text{avg}}^n = \frac{\min(\mathcal{T}_{i,j}^n) + \max(\mathcal{T}_{i,j}^n)}{2}$ # average time point of $\mathcal{T}_{i,j}^n$
    end for
  end for
  1. Based on $t_{i,j,\text{avg}}^n \forall n \in \{1, 2, 3\}$, evaluate all $p_i(t) \forall\, j \in \mathcal{D}^n$ up to conflict point $n = 3$.
  2. From step 1, for each $n \in \{1, 2, 3\}$ identify the disjoint set $\mathcal{T}_{i,j}^n$ which results in $p_i(t)$ that minimizes jerk.
  Output: $\mathcal{T}_i^{1*}, \mathcal{T}_i^{2*}, \mathcal{T}_i^{3*}$ based on the identified $j\ \forall\ n \in \{1, 2, 3\}$ from the previous step 2.

Proposition 1: Consider a CAV $i \in \mathcal{N}(t)$ and a preceding CAV $k \in \mathcal{N}(t) \setminus \{i\}$ on the same path $z \in \mathcal{L}$. If we enforce $\tau_r >= 2\tau_\ell$, where τ_r and τ_ℓ are defined in (4), (5) and (6), then for every conflict point $n \in \{1, 2, 3\}$ along path z, there exists a non-empty feasible time set $\mathcal{M}_n = [\underline{\tau}, \overline{\tau}] \neq \emptyset$, within which a CAV j from a path conflicting with path z can safely pass between the two CAVs i and k.

Proof: For conflict point n^* and an arbitrary moment consider without loss of generality t^{n^*} symmetrically between t_k and t_i. From proposition statement $\tau_r \ge 2\tau_\ell$ is met. Then $\tau_r \ge 2\tau_\ell \Rightarrow |t_k - t_i| \ge |t_k - t^{n^*}| + |t^{n^*} - t_i|$. Consequently, there exists t^{n^*} where a CAV j from a conflicting path can cross point n^* between CAVs k and i. This completes the proof. ■

Remark 3: We have ensured the existence of t_i^1, t_i^2, and t_i^3 for the lateral safety constraint. Given that the lateral constraints can only occur at points $(t_i^1, p_i^1), (t_i^2, p_i^2), (t_i^3, p_i^3)$, and given that the function $p_i(t)$ is strictly increasing, the final trajectory cannot make any of the lateral constraints active.

Remark 4: Proposition 1 enhances the feasibility of a CAV to navigate between two other CAVs from a conflicting path. While the inequality $\tau_r \ge 2\tau_\ell$ mandates that vehicles on the same path maintain a greater distance, this requirement, not included in [19], can broaden the practical applicability of our approach. This is because it ensures we can identify time points t_i^n that adhere to the lateral constraints.

D. Rear-End Constraints

Although we have proven that t_i^1, t_i^2, and t_i^3 can always be feasible to guarantee lateral constraints, we must also define conditions for the rear-end constraints. An analytical approach offering such a guarantee is non-trivial, given the polynomial's design through (10), and has not been explicitly addressed in the literature to date. In instances where rear-end constraints may become active, an approach similar to [23] (see Section IV-B) can be employed. Finally, our solution must also adhere to vehicle speed and acceleration constraints. Next, we discuss how these constraints can influence our solution approach.

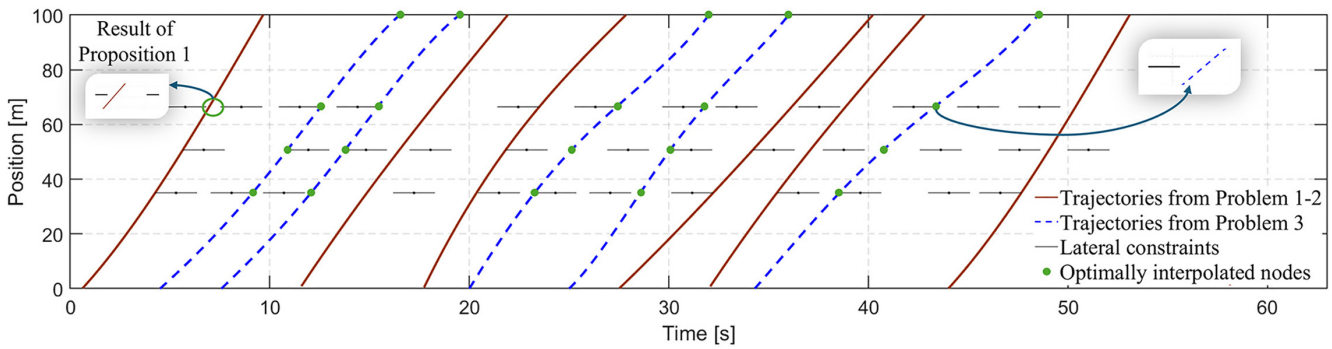

Fig. 2. Position trajectories on path 5.

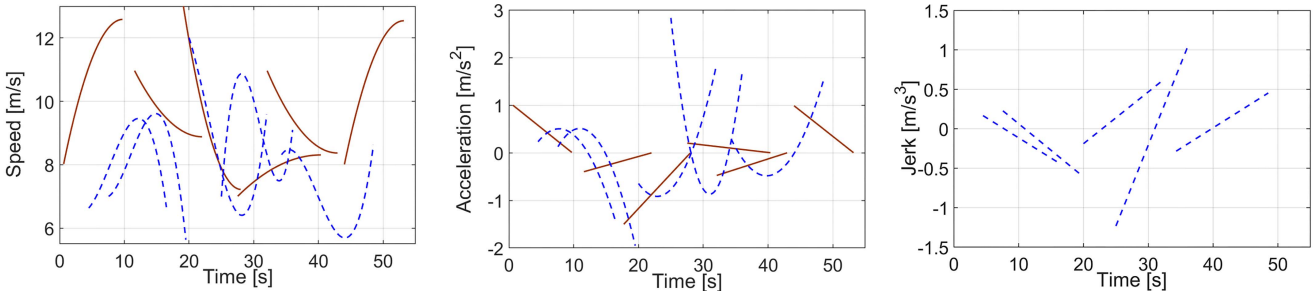

(a) Speed trajectories on path 5. (b) Acceleration trajectories on path 5. (c) Jerk trajectories on path 5.

Fig. 3. Speed, acceleration, and jerk trajectories on path 5.

E. Solution

In this subsection, we analyze the solution approach. Recall that we aim to minimize the jerk of the position trajectory. Therefore, let us define a function $g : \mathbb{R}^5 \rightarrow \mathbb{R}$ which takes as parameters the vector $\{t_i^0, t_i^1, t_i^2, t_i^3, t_i^f\}$, computes the fourth order polynomial trajectory $p_i(t)$ using (10) and returns the jerk of that polynomial, which is the third derivative of $p_i(t)$. So, we aim to find the optimal values of $t_i^1, t_i^2, t_i^3, t_i^f$ to minimize the jerk of CAV i. Recall that t_i^0 is known.

Before introducing the optimization framework that addresses this problem, we denote the feasible domain for each parameter t_i^n as $\mathcal{T}_i^n$, $n \in \{1, 2, 3, f\}$. Note that each $\mathcal{T}_i^n, n \in \{1, 2, 3\}$ consists of a union of disjoint compact time sets due to the existence of lateral constraints associated with the set of conflict points $\mathcal{O}_z = \{1, 2, 3\}$. For each conflict point $n \in \mathcal{O}_z$ we define the set $\mathcal{T}_i^n = \{\mathcal{T}_{i,1}^n, \mathcal{T}_{i,2}^n, \ldots, \mathcal{T}_{i,\mathcal{D}^n}^n\}$ where $\mathcal{D}^n$ defines the number of disjoint sets for conflict point n. For example, in Fig. 2, the first solid curve refers to the position trajectory of CAV i that passes through the disjoint sets $\mathcal{T}_{i,0}^1$, $\mathcal{T}_{i,0}^2$ and $\mathcal{T}_{i,1}^3$. So, we can think of these disjoint sets as the blank spaces between the black dashes that represent lateral constraints.

Conversely, the exit time t_i^f is subject to rear-end constraints or the lower bound $\underline{t}_i^f$ whichever is more restrictive, and the upper bound $\overline{t}_i^f$. This ensures that the set of feasible exit times, denoted as $\mathcal{T}_i^f$, forms already a compact set.

Considering all the disjoint sets in $\mathcal{T}_i^n$ for each conflict point $n \in \{1, 2, 3\}$ as the feasibility domain of t_i^n does not facilitate the optimization process. Consequently, our goal is to limit the feasibility set for each t_i^n to a single convex set. To achieve this, we need to select only one set among the multiple disjoint sets included in $\mathcal{T}_i^n$. For each CAV i and for each conflict point $n \in \mathcal{O}_z$, we introduce Algorithm 1 to select a single convex set $\mathcal{T}_i^{n*} \subseteq \mathcal{T}_i^n$, focusing on jerk minimization. The asterisk (*) is used to denote the selected disjoint set $\mathcal{T}_i^{n*}$.

Now that we have defined a convex feasible set for each t_i^n, we are in a position to present our minimization problem.

Problem 3

$$\min_{t_i^1, t_i^2, t_i^3, t_i^f} \int_{t_i^0}^{t_i^f} \left(g(t; t_i^0, t_i^1, t_i^2, t_i^3, t_i^f)\right)^2 dt \tag{12}$$

$$\text{subject to: } t_i^0 \text{ given, } t_i^1 \in \mathcal{T}_i^{1*},\ t_i^2 \in \mathcal{T}_i^{2*},\ t_i^3 \in \mathcal{T}_i^{3*},$$
$$t_i^f \in \mathcal{T}_i^{f*}, p_i\left(t_i^0\right) = p_i^0,\ v_i\left(t_i^0\right) = v_i^0,\ (1),\ (2),\ (3). \tag{13}$$

Give that the domain of each t_i^n forms a convex set, it streamlines the search process and facilitates the rapid acquisition of a numerical solution.

IV. Numerical Simulations

We conduct numerical simulations at an intersection as depicted in Fig. 1. Each path was set to a length of 100 m, with a speed limit of 17 m/s and acceleration limits of -5 m/s^2 and 5 m/s^2. The initial speeds of the vehicles were uniformly sampled from the interval [6 m/s, 15 m/s].

Fig. 2 displays the position trajectories for vehicles on path 5 under a traffic flow of 7000 veh/h from all entries. Observing the blue trajectories, it is evident that our system required five times the utilization of Problem 3 within a time interval of 53 seconds due to infeasibilities raised from Problems 1 and 2. The impact of this new approach is readily confirmed by comparing the speed and acceleration profiles from the prior and proposed approach in Figs. 3(a) and 3(b). Thanks to the utilization of a higher-order polynomial, the speed trajectories can change slope sign even two times while the acceleration profiles can attain non-linear shapes. For instance, by observing the CAV that entered the intersection at $t = 25$ s, we can verify in Fig. 3(a) that it follows a speed trajectory where the slope starts positive, then becomes negative, and finally turns positive again. This also confirms the discussion in Lemma 1. Simultaneously, in Fig. 3(b) the acceleration is

TABLE I
PERCENTAGE OF SUCCESSFUL TRIALS AMONG 50 SIMULATIONS BETWEEN THE TWO APPROACHES

Traffic Volume (veh/h)	Percentage of successful trials	
	Prior Approach	Proposed Approach
3000	100%	100%
4000	92%	100%
5000	76%	100%
6000	34%	52%
7000	0%	28%

non-linear while remains within the boundary limits, ensuring a natural driving experience.

The solutions from Problem 3 result in linear jerk trajectories, as shown in Fig. 3(c). Note that only vehicles utilizing Problem 3 display non-zero jerk, whereas vehicles that use Problem 2 follow a third order polynomial path with zero jerk. Consequently, their jerk trajectories are omitted.

Regarding Proposition 1, we verify its applicability by observing Fig. 2. Specifically, in the upper left corner, we zoomed on a frame confirming the result. Recall this proposition mandates sufficient distance between vehicles on the same path to ensure safe passage from vehicles on conflicting paths.

Our study also included a quantitative analysis aimed at evaluating the efficacy of the two approaches for five different traffic volumes. For each of the five distinct traffic volumes considered, we conducted 50 individual simulations, each lasting 300 seconds. These simulations were initialized with varying seed values to capture a range of initial conditions. We recorded the number of simulations that finished successfully, indicating that all CAVs identified feasible trajectories.

Our results, illustrated in Table I, demonstrate a significant performance improvement with our proposed approach over the prior method. Notably, using our approach, even with a traffic volume of 5000 veh/h, all CAVs successfully navigated through the intersection in each of the 50 simulations. In contrast, employing the previous approach resulted in only 76 % of simulations achieving the same level of success, underscoring a performance increase of 31.5%, under the same traffic conditions. Above this threshold, at 6000 veh/h, our approach continued to outperform the prior one. Finally, at 7000 veh/h, the prior approach failed to find feasible solutions in every simulation, whereas our approach maintained a success rate of 28%. Supplementary material is available on this letter's website at: https://sites.google.com/cornell.edu/feasibility.

V. CONCLUDING REMARKS

In this letter, we addressed the problem of expanding the feasible solution domain within a decentralized control framework for CAVs at signal-free intersections. The proposed approach employs numerical interpolation techniques to establish a feasible trajectory for CAVs crossing a signal-free intersection. Our findings demonstrate that our approach can significantly extend the feasibility domain and provide a real-time solution. This result is worth considering for dense urban networks, circumventing the feasibility limitations in [19].

Despite a polynomial solution's ability to satisfy rear-end and lateral constraints, it was expected that higher traffic volumes might result in no combination of interpolated nodes that satisfy speed and acceleration constraints. So, a valuable direction for future research is finding conditions on the arrival times that guarantee constraint satisfaction. For example, this may be achieved using Lipschitz continuity (see [24]). Another potential direction for future research is generalizing this method within mixed-traffic environments. Finally, given the efficiency of our approach, it would be worthwhile to explore the applicability of numerical interpolation in other optimal control applications, such as robots / micro-robots navigation.

REFERENCES

[1] J. Chow, *Informed Urban Transport Systems: Classic and Emerging Mobility Methods Toward Smart Cities*. Amsterdam, The Netherlands: Elsevier, 2018.

[2] J. Guanetti, Y. Kim, and F. Borrelli, "Control of connected and automated vehicles: State of the art and future challenges," *Annu. Rev. control*, vol. 45, pp. 18–40, Jan. 2018.

[3] Y. Du, M. A. Makridis, C. M. Tampère, A. Kouvelas, and W. ShangGuan, "Adaptive control with moving actuators at motorway bottlenecks with connected and automated vehicles," *Transp. Res. Part C, Emerg. Technol.*, vol. 156, Nov. 2023, Art. no. 104319.

[4] N. Shiwakoti, P. Stasinopoulos, and F. Fedele, "Investigating the state of connected and autonomous vehicles: A literature review," *Transp. Res. Procedia*, vol. 48, pp. 870–882, Jan. 2020.

[5] L. Xiao and F. Gao, "A comprehensive review of the development of adaptive cruise control systems," *Veh. Syst. Dyn.*, vol. 48, no. 10, pp. 1167–1192, 2010.

[6] R. A. Dollar and A. Vahidi, "Efficient and collision-free anticipative cruise control in randomly mixed strings," *IEEE Trans. Intell. Veh.*, vol. 3, no. 4, pp. 439–452, Dec. 2018.

[7] D. Schrank, B. Eisele, T. Lomax, and J. Bak, *Urban Mobility Scorecard*, Texas A&M Transp. Inst., College Station, TX, USA, 2015.

[8] W. Xiao and C. G. Cassandras, "Decentralized optimal merging control for connected and automated vehicles with safety constraint guarantees," *Automatica*, vol. 123, Jan. 2021, Art. no. 109333.

[9] V.-A. Le, B. Chalaki, F. N. Tzortzoglou, and A. A. Malikopoulos, "Stochastic time-optimal trajectory planning for connected and automated vehicles in mixed-traffic merging scenarios," 2023, *arXiv:2311.00126*.

[10] A. Katriniok, "Towards learning-based control of connected and automated vehicles: Challenges and perspectives," *AI-enabled Technologies for Autonomous and Connected Vehicles*. Cham, Switzerland: Springer, 2022, pp. 417–439.

[11] K. Katzilieris, E. Kampitakis, and E. I. Vlahogianni, "Dynamic lane reversal: A reinforcement learning approach," in *Proc. 8th Int. Conf. Models Technol. Intell. Transp. Syst. (MT-ITS)*, 2023, pp. 1–6.

[12] R. Hult, M. Zanon, S. Gros, and P. Falcone, "Optimal coordination of automated vehicles at intersections: Theory and experiments," *IEEE Trans. Control Syst. Technol.*, vol. 27, no. 6, pp. 2510–2525, Nov. 2019.

[13] B. Alrifaee, "Networked model predictive control for vehicle collision avoidance," Ph.D. dissertation, Dept. Mech. Eng., RWTH Aachen Univ., Aachen, Germany, 2017.

[14] A. E. Bryson, *Applied Optimal Control: Optimization, Estimation and Control*. New York, NY, USA: Routledge, 2018.

[15] P.-C. Aubin-Frankowski, "Linearly constrained linear quadratic regulator from the viewpoint of kernel methods," *SIAM J. Control Optim.*, vol. 59, no. 4, pp. 2693–2716, 2021. [Online]. Available: https://doi.org/10.1137/20M1348765

[16] J. Rios-Torres and A. A. Malikopoulos, "Automated and cooperative vehicle merging at highway on-ramps," *IEEE Trans. Intell. Transp. Syst.*, vol. 18, no. 4, pp. 780–789, Apr. 2017.

[17] Y. Zhang, C. G. Cassandras, and A. A. Malikopoulos, "Optimal control of connected automated vehicles at urban traffic intersections: A feasibility enforcement analysis," in *Proc. Am. Control Conf. (ACC)*, 2017, pp. 3548–3553.

[18] A. M. I. Mahbub and A. A. Malikopoulos, "Conditions to provable system-wide optimal coordination of connected and automated vehicles," *Automatica*, vol. 131, Sep. 2021, Art. no. 109751.

[19] A. A. Malikopoulos, L. E. Beaver, and I. V. Chremos, "Optimal time trajectory and coordination for connected and automated vehicles," *Automatica*, vol. 125, Mar. 2021, Art. no. 109469.

[20] A. Quarteroni, R. Sacco, and F. Saleri, *Numerical mathematics*, vol. 37, New York, NY, USA: Springer, 2006.

[21] Z. Shen and K. Serkh, "Polynomial interpolation in the monomial basis is stable after all," 2023, *arXiv:2212.10519*.

[22] L. E. Beaver, "LQ-OCP: Energy-optimal control for LQ problems," 2023, *arXiv:2310.00168*.

[23] H. Bang and A. A. Malikopoulos, "Optimal trajectory planning meets network-level routing: Integrated control framework for emerging mobility systems," 2023, *arXiv:2311.13193*.

[24] H. K. Khalil, *Control of Nonlinear Systems*. New York, NY, USA: Prentice-Hall, 2002.